The Canadian Mineralogist
Vol. 32, pp. 307-317 (1994)

SIGNS OF INCONGRUENT MELTING OF CLINOPYROXENE IN LIMBURGITE, THETFORD HILL, VERMONT

M.J. HIBBARD

Department of Geological Sciences, University of Nevada, Reno, Nevada 89557, U.S.A.

JAMES J. SJOBERG

U.S. Bureau of Mines, Reno Research Center, 1605 Evans Avenue, Reno, Nevada 89512, U.S.A.

ABSTRACT

Phenocrysts of augite in a limburgite from the Thetford Hill area of Vermont contain a textural and compositional record of resorption (dissolution melting) and incongruent direct melting. Early magmatic crystallization of phenocryst-size sodian augite and olivine was followed by partial dissolution melting of the sodian augite at phenocryst–melt interfaces and incongruent melting within the sodian augite phenocrysts, both attendant to drastic reduction in geostatic pressure resulting from intrusion. The dissolution melting resulted in rounded phenocrysts, whereas the incongruent direct melting produced a spongy framework of sodian augite and a melt chemically equivalent to non-sodian augite, plagioclase, olivine, and titaniferous magnetite. The sodian augite was transformed to non-sodian augite by diffusional exchange of Na, Fe, and Mg (into the melt) for calcium (into the solid phase). In addition, the spongy framework was locally cross-cut by microveins containing epitaxic boxy-lamellar non-sodian augite, crystallizing from local, not ambient melt. Both the matrix and intraphenocryst mineral assemblages consist of non-sodian augite, plagioclase, olivine, and titaniferous magnetite. The ambient melt was of slightly different composition than the intraphenocryst melt, as indicated by the growth of a titanaugite rim on (1) the surfaces of augite phenocrysts in contact with ambient melt, and (2) the augite crystals in the matrix. Significantly, lack of a titaniferous rim on augite within phenocrysts indicates that melt generated by incongruent melting did not mix physically nor chemically with the ambient melt.

Keywords: limburgite, dissolution, incongruent melting, augite, magmatic crystallization, Vermont.

SOMMAIRE

Des phénocristaux d'augite dans une limburgite de la région de Thetford Hill, au Vermont, témoignent d'une dissolution par résorption et d'une fusion incongruente, tant par leur texture que par leur composition. Une cristallisation précoce de phénocristaux d'augite sodique et d'olivine a été suivie par une dissolution partielle de l'augite à l'interface phénocristal–liquide, et d'une fusion incongruente de l'intérieur des phénocristaux, en réponse à une réduction brutale de la pression géostatique suite à la mise en place. La résorption a donné des phénocristaux arrondis, tandis que la fusion inconguente a produit une trame spongieuse et un liquide chimiquement équivalent à un mélange d'augite non sodique, plagioclase, olivine et magnétite titanifère. L'augite sodique a été transformée en augite sans Na par échange de Na, Fe et Mg avec le liquide par diffusion; par contre, le Ca s'est concentré dans le pyroxène. De plus, la trame spongieuse est recoupée par des veinules contenant un enboîtement lamellaire épitaxique d'augite non sodique, formé à partir d'un liquide localisé, et non du liquide ambiant. La pâte et l'assemblage de minéraux intraphénocristaux contiennent augite non sodique, plagioclase, olivine et magnétite titanifère. Le liquide ambiant avait une composition légèrement différente du liquide intraphénocristal, comme en témoigne la croissance d'un liseré de titanaugite sur 1) la surface des phénocristaux d'augite en contact avec le liquide ambiant, et 2) la bordure des grains d'augite de la pâte. L'absence de bordure titanifère sur l'augite à l'intérieur des phénocristaux montre que le liquide interne formé par fusion incongruente ne s'est pas mélangé physiquement ou chimiquement avec le liquide ambiant.

(Traduit par la Rédaction)

Mots-clés: limburgite, dissolution, fusion incongruente, augite, cristallisation magmatique, Vermont.

INTRODUCTION

In those magmatic systems subject to a drastic change in geostatic pressure attendant to intrusion, or to an extreme thermal contrast resulting from magma mixing, or to both of these occurring simultaneously, there is likely to be a mineralogical and textural expression of episodic resorption or dissolution (crystal dissolves into an ambient melt undersaturated in the crystal phase) and perhaps of direct melting (new melt forms directly from a crystal phase). The challenge has been to distinguish those textures that are indicative of crystal growth from those resulting from dissolution and direct melting, and, furthermore, to track the mechanism of development of a new solid phase in the case of incongruent direct melting (Tsuchiyama & Takahashi 1983, Tsuchiyama 1985, Kuo & Kirkpatrick 1985, Donaldson 1985, O'Brien

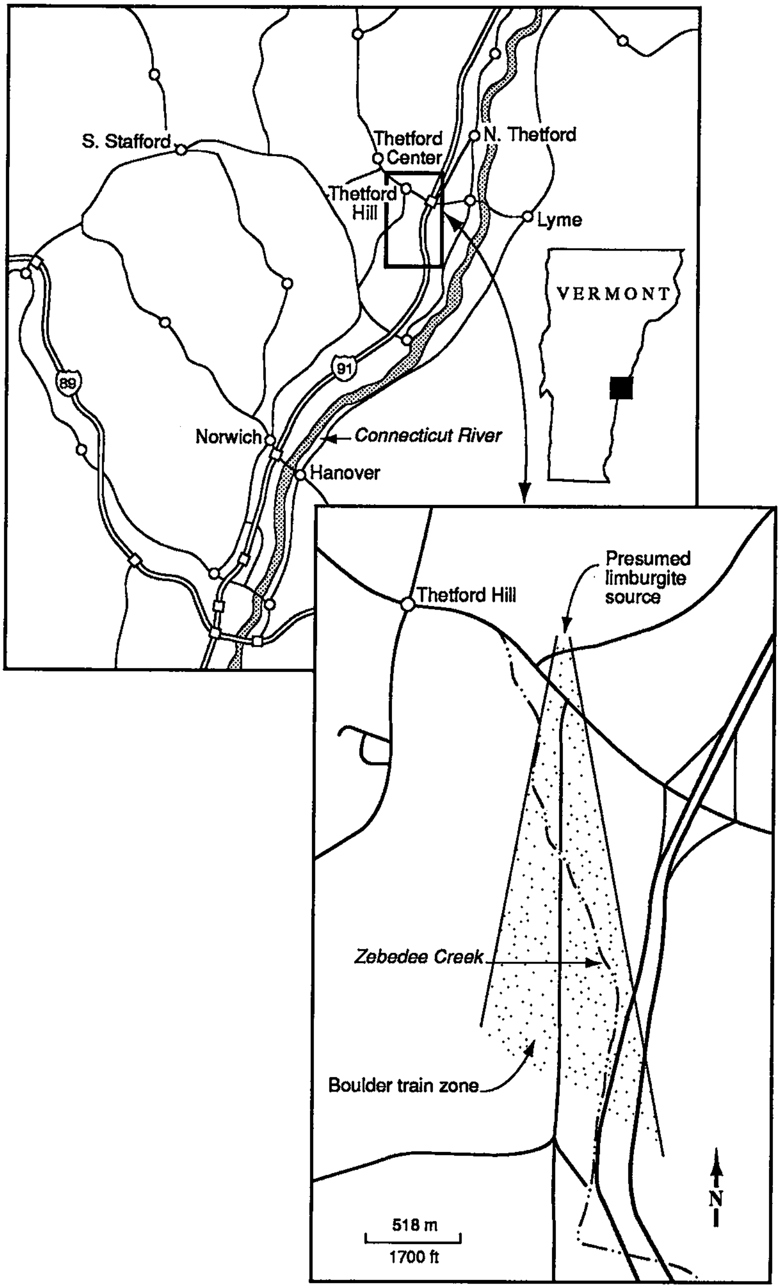

FIG. 1. Location map of limburgite in boulder train (mostly relocated into stone walls) near Thetford Hill, Vermont. After Warren Chivers.

et al. 1988, Nelson & Montana 1992). Volcanic rocks are particularly well suited for such investigations because changes in confining pressure during crystallization are likely to be extreme and, therefore, textural expression of pressure change and its effect on the position of liquidi and solidi can be expected to be pronounced.

Clinopyroxene occurring in a limburgite collected from a stone fence, located between good neighbors in the Thetford Hill area, Vermont (Fig. 1, no outcrops), presents an opportunity to characterize textures that distinguish between (1) early magmatic growth of crystals, (2) an episode of resorption (dissolution melting), (3) an episode of incongruent direct melting, and (4) a second and final stage of magmatic crystal-growth.

THE LIMBURGITE

The Thetford limburgite contains clinopyroxene and olivine phenocrysts, a few centimeters in diameter, occurring in a fine-grained (0.2 mm) matrix (Fig. 2). The matrix mineral assemblage consists of olivine (Fo_{66}, largely but not completely replaced by septechlorite), augite zoned to a titanaugite rim, calcic plagioclase (normally zoned without oscillations, An_{65-55}), titaniferous magnetite, and a few patches of carbonate. The olivine phenocrysts also are partially altered to septechlorite.

Clinopyroxene phenocrysts typically consist of (1) noncellular light brown augite (light grey in hand specimen), (2) epitaxic clear cellular augite (black in hand specimen), and (3) a lilac-colored epitaxic titanaugite rim. Except for the atypical presence of plagioclase (10% by volume), this mineral assemblage typically corresponds to those alkaline volcanic rocks associated with alkali basalts known as limburgite (Wilkinson 1974). It is not presently known how the Thetford limburgite relates to other mafic and alkaline mafic rocks in New England (McHone 1978, Leavy & Hermes 1979). The regional geology has been mapped by Hadley (1950).

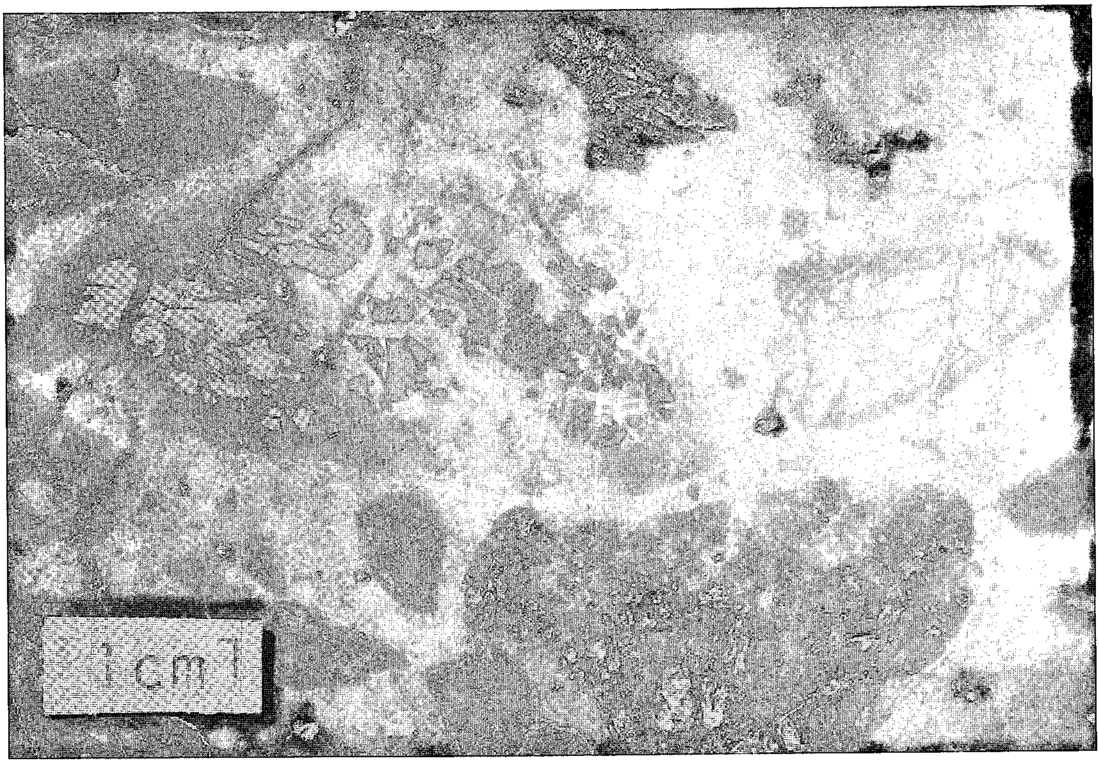

FIG. 2. Slabed hand specimen of limburgite. Large rounded phenocryst (center left) consists of cellular non-sodian augite (darker) occurring as a "mantle" on and as "veinlets" in relict noncellular sodian augite (lighter). Large rounded phenocryst (lower right) is olivine partly replaced by septechlorite.

THE PYROXENE

There are four morphologically distinct types of augite constituting phenocrysts: (1) noncellular sodian augite, (2) fine spongy cellular augite, (3) coarse boxy-lamellar cellular augite, and (4) noncellular augite zoned to titanaugite interfacing with the matrix (Figs. 3A–D). "Cellular" is used here in a nongenetic sense to describe incomplete crystal morphology characterized by "cells" that contain different mineral phases than the host crystal. The cells may be isolated or interconnecting, and their surfaces may be rounded or facet-like. In this sense, the "spongy cellular" texture consists of an interconnected crystalline framework in which there is a linking of rounded crystalline phase and a corresponding interconnection of cells.

The noncellular augite is inclusion-free, occurring primarily in the core of phenocrysts, but also as "fragments" that at least appear to be isolated in cellular augite of the phenocrysts (Fig. 2). It is sodian augite ($2V_z$ 55°) having a significantly larger Na content than the cellular augite (Table 1). It is similar to the clinopyroxene reported by Binns (1969) to occur in some basanites.

The fine spongy cellular augite dominates the outer portion of the phenocrysts as a crude "mantle", and it also occurs along cleavage directions extending toward the interior of the phenocrysts (Fig. 3D). A similar texture in augite is shown by Tsuchiyama & Takahashi (1983, Fig. 11B). The spongy augite is epitaxic with noncellular sodian augite. Plagioclase (An_{41}, Table 1), septechlorite (presumably after olivine), and titaniferous magnetite occur in the "cells" of the augite, as shown in the SEM-generated backscattered electron image (Fig. 4B) and the photomicrograph (Fig. 5A).

The boxy-lamellar cellular augite is of a larger "grain-size" than the spongy cellular augite (Figs. 3C, 5C), appearing lamellar in longitudinal section and somewhat boxy in cross section (especially Fig. 5C). It is epitaxic with both the noncellular host augite and the fine spongy cellular augite. Boxy-lamellar cellular

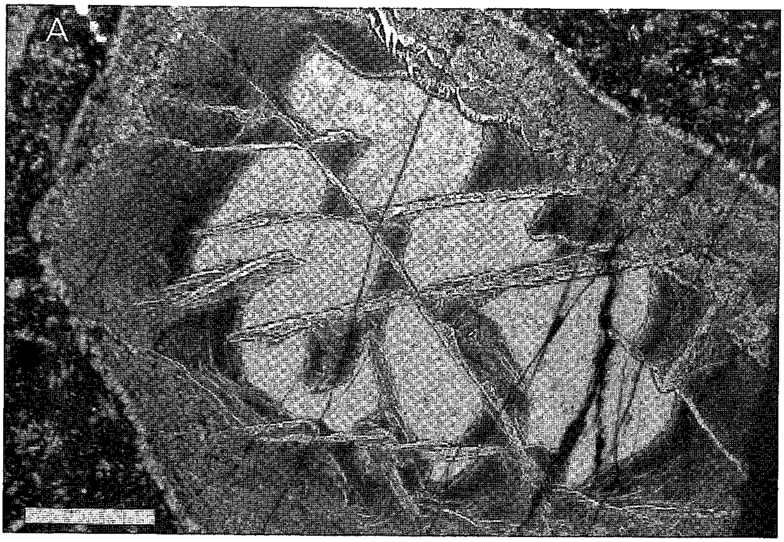

FIG. 3. The different components of the augite phenocrysts. (A) Relict noncellular sodian augite core cross-cut by microveins of epitaxic boxy-lamellar cellular non-sodian augite parallel to the two directions of cleavage of the pyroxene. Finer spongy cellular non-sodian augite "mantles" the core complex but also occurs as patches within the core. Narrow rim of titanaugite interfaces with matrix mineral assemblage. Post-crystallization NNE-SSW fractures are roughly parallel to {010}. Bar scale: 1 mm. (B) Sharp contacts of "mantle" and "microvein" cellular non-sodian augite in relation to noncellular sodian augite. Note sharp and gradational (upper left) relation of coarse boxy-lamellar augite to fine spongy augite. Bar scale: 0.5 mm. (C) From left to right: coarse boxy-lamellar cellular augite, spongy cellular augite, coarse augite zoning to titanaugite facing matrix. A few of the grains of titaniferous magnetite are shown with white arrows, and the remaining black "cells" contain plagioclase and septechlorite pseudomorphic after olivine. Spongy cellular augite associated with coarse elongate variety shown with black arrow. Bar scale: 0.25 mm. (D) Spongy cellular augite "mantle" with "microvein" extensions into interior of phenocryst parallel to cleavage. Note titanaugite rim. Bar scale: 0.5 mm.

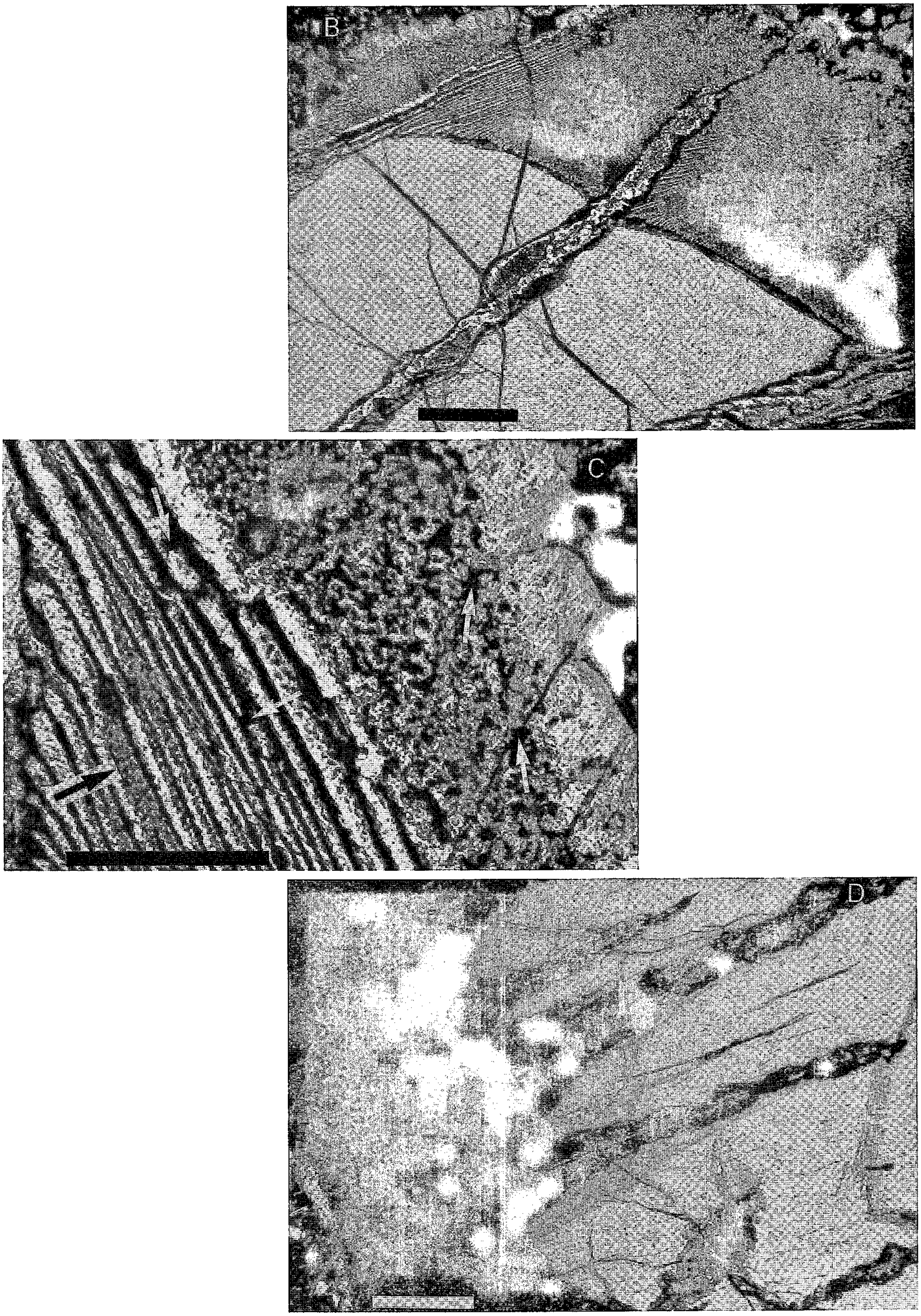
B
C
D

TABLE 1. RESULTS OF SEM SEMIQUANTITATIVE ANALYSIS OF AUGITE AND ASSOCIATED MINERALS IN LIMBURGITE, THETFORD HILL, VERMONT

	NC Cpx (2)	SP Cpx (2)	BL Cpx (3)	Rim Cpx (3)	Pl mtx (2)	Ol mtx (2)	Ti Mag (2)
SiO_2	52.90	53.20	52.80	48.00	59.58	38.92	
TiO_2	0.60	0.40	0.69	2.38			23.66
Al_2O_3	6.70	3.00	4.70	6.63	26.30		
FeO^*	6.64	5.37	5.80	6.58		17.40	71.85
MnO	0.09	0.19	0.22	0.10			
MgO	15.70	17.60	18.00	13.00		43.32	4.49
CaO	15.50	19.80	16.90	22.40	7.78	0.36	
Na_2O	1.55	0.02	0.50	0.10	6.08		
K_2O	0.05	0.10	0.16	0.08	0.26		

calculated formulas:

NC Cpx: non-cellular clinopyroxene
$Mg_{0.85}Ca_{0.61}Fe_{0.2}Al_{0.2}Na_{0.11}Ti_{0.01}(Al_{0.08}Si_{1.9})O_6$

SP Cpx: spongy cellular clinopyroxene
$Mg_{0.96}Ca_{0.77}Fe_{0.16}Al_{0.07}Ti_{0.01}(Al_{0.06}Si_{1.94})O_6$

Ol mtx: olivine in matrix
$Mg_{1.64}Fe_{0.37}Ca_{0.01}Si_{0.99}O_4$ (Fo_{66})

Pl mtx: plagioclase in cellular augite
$Na_{0.53}Ca_{0.37}Al_{1.4}Si_{2.6}O_8$ (An_{41})

Ti Mag: titaniferous magnetite in boxy-lamellar clinopyroxene (BL Cpx)
$Fe_{1.8}Ti_{0.5}Mg_{0.2}O_4$

The analyses were made on selected points on a polished thin section (Fig. 4B) with analyzed mineral samples and pure metals used as standards. The analyses were performed at the U.S. Bureau of Mines, Reno Research Center, using a JEOL T-300 scanning electron microscope equipped with a PGT System 4 X-ray analyzer. * Total iron expressed as FeO. (#) number of points analyzed. Results quoted in weight %.

augite typically occurs as "microveins" (Figs. 3A, B, 5B, C) corresponding to cleavage directions (Fig. 3A) and what may have been fracture and shear directions. There is local textural gradation between boxy-lamellar and fine spongy cellular augite (Figs. 3A, B, C, 5B, C). Elongate cells of the boxy-lamellar augite contain the same plagioclase, septechlorite (olivine), and titaniferous magnetite present in the fine spongy cellular augite.

INTERPRETATION OF CELLULAR AUGITE

Chemical relations

The difference in Na content between noncellular and both the fine spongy and the coarse boxy-lamellar cellular augite is readily apparent (Table 1). Since there are no inclusions of septechlorite (olivine), plagioclase, or titaniferous magnetite in the noncellular sodian augite, this mineral assemblage must have been generated at the same time as the cellular augite if a closed chemical system can be demonstrated. An equation relating the primary noncellular augite to the generation of cellular augite and coexisting plagioclase, olivine (presumed) and titaniferous magnetite is as follows: 25 sodian augite → 18 augite + 3 olivine (Fo_{66}) + 3 plagioclase (An_{41}) + 1 titaniferous magnetite.

The proportions of minerals shown in the equation, as permitted by mineral chemistry (Table 1), correlate fairly well with both an optical mode-count and a back-scattered electron image analysis (Table 2). Considering the inaccuracy of determining an optical mode in such fine-grained material, the probability of chemical mobility during the crystallization of the reaction products, as well as the morphological anisotropy (especially the boxy-lamellar cellular augite) as governed by orientation of the thin section, the results are considered to be compatible with the notion that there was generation of augite, olivine, plagioclase, and titaniferous magnetite by reorganization of chemical components of the sodian augite, without significant (if any) chemical interaction with the ambient magma.

Textural relations

Assuming that the limburgite is fundamentally a product of magmatic crystallization, based on the phenocryst–matrix textural relations and the growth of many crystals in the matrix terminating with crystal faces, the creation of four mineral phases at the expense of a single mineral phase can be explained in this magmatic context by incongruent direct melting related to an episode of pressure change.

Partial dissolution melting (resorption) of phenocrysts is suggested by the rounded character of the phenocrysts (Figs. 2, 6) (see also Kuo & Kirkpatrick 1985), although a component of mechanical wear cannot be ruled out. Rapid decompression as a consequence of intrusion is a well-known mechanism of lowering liquidi and solidi, with consequent dissolution melting or direct melting (Nelson & Montana 1992). Since there is no evidence of magma mixing preserved in the limburgite, reheating by that mechanism to initiate dissolution melting is ruled out in this case.

Incongruent direct melting is suggested also to have occurred in response to rapid decompression, leading eventually to the development of cellular non-sodian augite from original noncellular sodian augite (Fig. 6). Incongruent melting theoretically generates a new solid phase and a melt, both of which are of different composition than the original solid phase. Just how the new solid phase originates is rarely characterized from a physical point of view. There are at least three possibilities: (1) nucleation and growth of the new solid phase in the melt in the vicinity of the former solid phase, (2) epitaxic crystallization of the new phase on the original solid phase, and (3) diffusional exchange between the original solid phase and the new

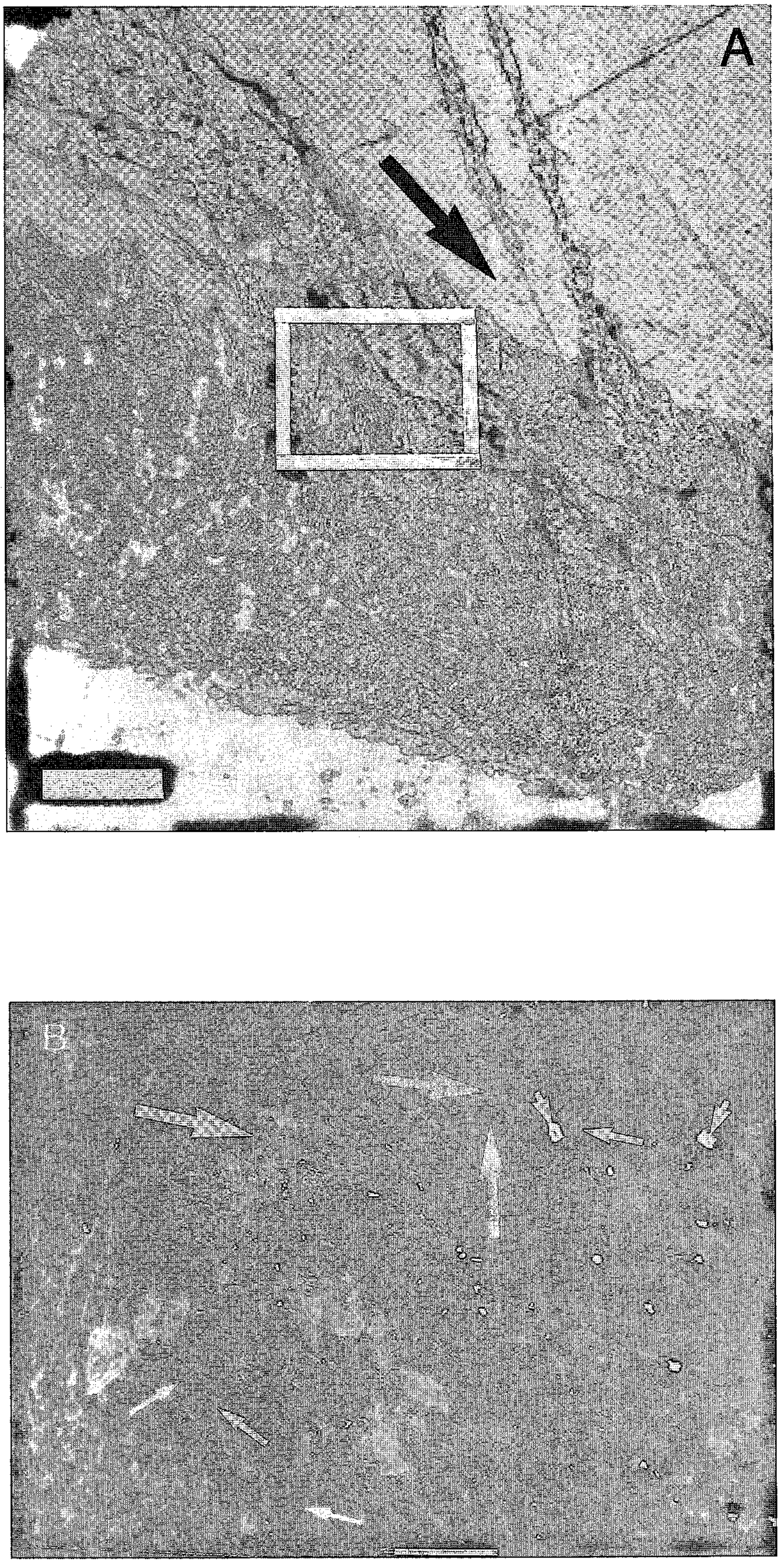

FIG. 4. (A) Photomicrograph of noncellular and cellular augite, showing location of SEM analysis of noncellular sodian augite (black arrow) and area shown in SEM back-scattered electron image in B. Bar scale: 0.5 mm. (B) SEM back-scattered electron image of cellular augite. Coarser boxy-lamellar cellular augite (upper right), finer spongy cellular augite (lower left). Darkest grey is area of septechlorite (large white arrow), medium grey is plagioclase (An_{41}) (two medium-sized white arrows indicate spots analyzed), white is titaniferous magnetite (two small white arrows indicate spots analyzed). Cellular spongy augite (medium-sized black arrows indicate spots analyzed) and coarser cellular augite (large black arrows indicate spots analyzed) make up the dominant phase (light grey). See Table 1 for compositions. Bar scale: 100 μm.

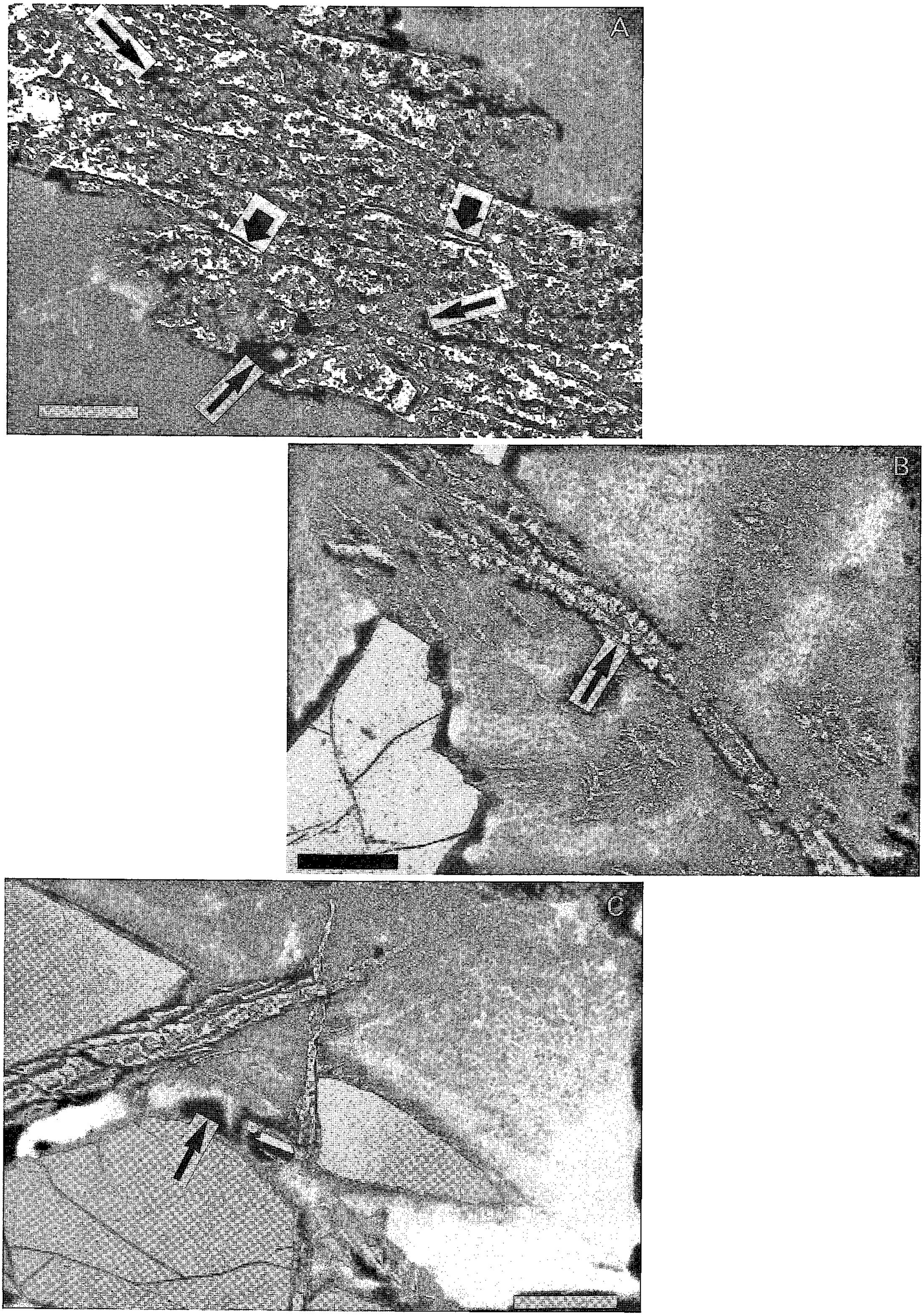
A
B
C

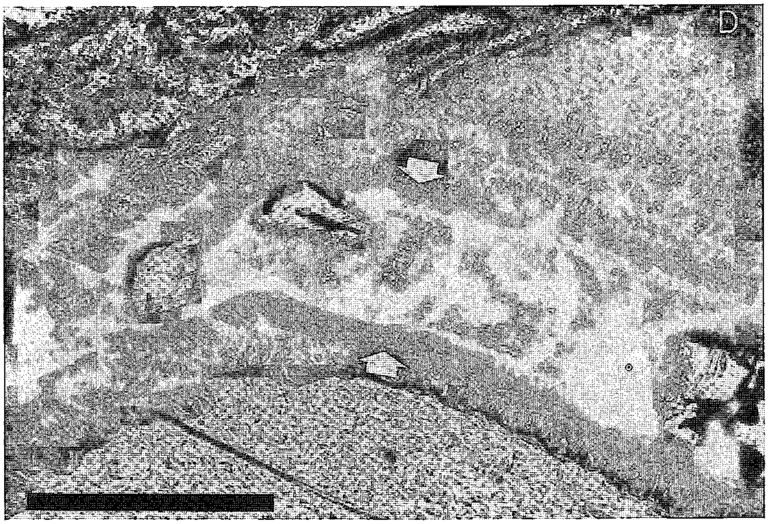

FIG. 5. (A) Photomicrograph showing grains of titaniferous magnetite (thin arrows) and plagioclase + septechlorite (thick arrows) occurring only in "microvein" of cellular augite in noncellular sodian augite (upper right and lower left). Bar scale: 0.05 mm. (B) Cross-cutting relation of mostly coarse boxy-lamellar cellular augite (arrow) to fine spongy cellular augite and to noncellular sodian augite (white). All three habits of augite are in optical continuity. Bar scale: 0.5 mm. (C) Late-stage mechanical separation of augite along cleavage (arrow) filled with matrix minerals and epitaxic titanaugite on cellular augite. Note two "microveins" of coarse boxy-lamellar cellular augite with adjacent noncellular sodian augite and fine spongy cellular augite. Bar scale: 0.5 mm. (D) Close-up of separation zone shown in (C). Titanaugite rim on spongy cellular augite (white arrows). Titanaugite rim on boxy-lamellar cellular augite (far left). Bar scale: 0.25 mm.

melt, driven by a chemical disequilibrium developed in response to, for example, a change in total pressure.

The cellular augite textures are interpreted to result from direct melting of sodian augite at high-energy sites, such as at dislocations and along grain, cleavage, fracture, or shear surfaces. Similar spongy cellular morphology has been produced in plagioclase by experimental melting (Tsuchiyama & Takahashi 1983, Nelson & Montana 1992) and observed in natural pyroxenes (O'Brien *et al.* 1988). The partial melting of noncellular sodian augite is envisioned as a progressive process, starting at the external surface of the sodian augite phenocrysts, probably already modified by dissolution melting (resorption), moving inward toward the core, but also laterally from fracture and cleavage surfaces that extend into the phenocrysts. Sites where melting had begun became the kinetically favored location of further progressive melting.

TABLE 2. PROPORTIONS OF REACTION PRODUCTS FORMED FROM SODIAN AUGITE, AS PREDICTED FROM MODEL CHEMICAL REACTION AND MEASURED FROM POINT-COUNT AND BACK-SCATTERED ELECTRON IMAGE COUNT

Reaction products	From est. equation (% formula units)	Optical mode (1000 counts in 1 mm² area) (area %)	High-resolution back-scattered electron image (0.25 mm² area) (area %)
Augite	72	79	74
Plagioclase	12	6	17
Olivine (as septechlorite)	12	9	8
Titaniferous magnetite	4	5	1

Since the cellular augite is of different composition than the original sodian augite, what must have been momentarily a spongy cellular sodian augite was converted to the non-sodian spongy augite. This is one style of incongruent melting, and its mechanism is proposed to be as follows. New nucleation and growth of non-sodian augite from cell melt of the cellular sodian augite, or epitaxic armoring of a cellular sodian augite with non-sodian augite, are precluded in view of the fact that the composition of the cellular augite is entirely sodium-free. Subsolidus homogenization of what might have been zoned augite, such as one with a sodian augite core and a non-sodian augite rim, is no

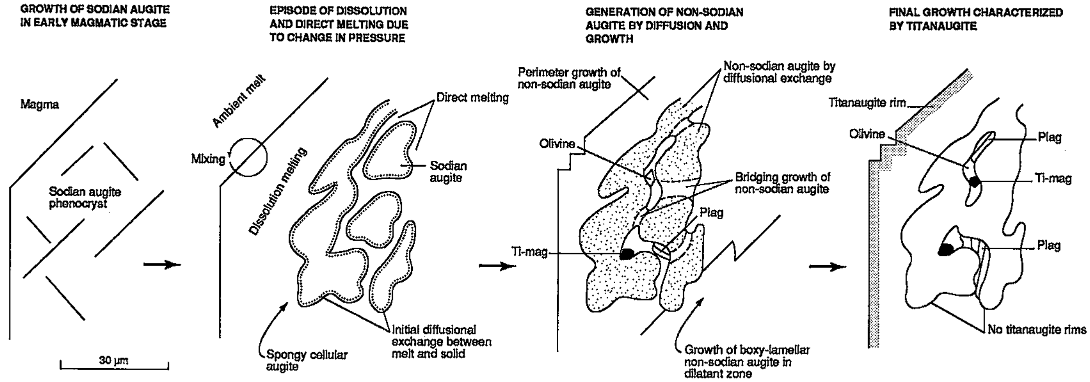

FIG. 6. Schematic representation of the derivation of spongy cellular non-sodian augite and boxy-lamellar cellular non-sodian augite from noncellular sodian augite phenocryst in the Vermont limburgite.

more likely here than in plagioclase of plutonic rocks, in which delicate oscillatory zoning typically is perfectly preserved.

Alternatively, it is proposed that the non-sodian cellular augite formed (1) partly from diffusional exchange and (2) partly from melt crystallization (Fig. 6). Unmelted cellular sodian augite is considered to have been modified by diffusional exchange of Na, Fe, and Mg (out of the crystal into the cell melt) for calcium (into the crystal from the melt). In this way, the Na-depleted cellular augite was generated. Similar diffusional adjustment between solid and melt is indicated for plagioclase (Tsuchiyama & Takahashi 1983).

The coarse boxy-lamellar cellular augite typically occurs as microveins, suggesting that its formation is governed by dilation along fractures, cleavages, or shears. Cell melt capable of diffusional exchange with sodian augite forming a non-sodian augite is also capable of crystallizing non-sodian augite of the same composition, as long as the system is chemically closed. There probably was epitaxic growth of non-sodian augite on diffusion-modified augite, perhaps bridging between granular portions of the spongy cellular framework and increasing the "grain size" of the framework (Fig. 6). Fluid concentration in zones of dilation led to the growth of the coarser boxy-lamellar augite. Thus non-sodian cellular augite is generated by both crystal growth and diffusional modification of a solid phase.

The question arises as to the possibility that all non-sodian cellular augite originated entirely by crystal growth. This model requires that the spongy cellular texture be a growth texture, not one of partial melting. Cellular crystal-growth is typically either boxy with development of crystal faces (Lofgren 1974), or dendritic, with characteristic arms and tip. The spongy cellular augite of the limburgite is characterized by rounded surfaces and nondendritic form. Even the boxy-lamellar cellular augite does not have dendritic morphology. Nevertheless, these observations do not necessarily preclude direct growth of spongy (sieve) crystals from melt (after all, the arms and tips of dendrites typically are rounded), but in the face of some uncertainty in this respect, and in the light of final growth of titanaugite from the ambient melt but not from the cell melt (next section), the model of incongruent melting involving diffusional modification, accompanied by crystallization from cell melt, is preferred.

LATE-STAGE FRACTURING AND MATRIX QUENCHING

Continuation of dynamic events in the evolution of the limburgite is indicated by fracturing and displacement of augite fragments after the formation of cellular augite. Dilation across fractures or cleavages allowed influx of the ambient melt, along with any crystals it may have contained at that time (Figs. 5C, D). Relatively rapid crystallization of ambient melt to non-sodian augite, plagioclase, olivine, and titaniferous magnetite, characterizing the matrix of the porphyritic rock, was more-or-less paralleled by growth of these same minerals from cell melt within the cellular augite. Very significantly, augite crystallizing in the matrix and as a noncellular rim on the exterior of phenocrysts is zoned outward to titanaugite (Figs. 3A, B, C, D, 5D), whereas no such zoning occurs within cellular augite of the phenocrysts (Fig. 6). This fact indicates that the melt within the cellular augite was generated *in situ* by direct melting and did not physically nor chemically mix with the ambient melt. If all of the cellular augite were a product of direct crystallization from ambient magma, zoning to a titanaugite rim would be expected within the cellular regions.

INTERPRETATION OF ENVIRONMENTAL EFFECTS

A model of evolution of the mineralogical and textural relations characterizing this limburgite is proposed as follows. Initial crystallization of augite and olivine phenocrysts occurred in a magma of alkali basaltic composition, in the upper mantle or lower crust. This was followed by a rapid reduction of confining pressure attendant upon intrusion to higher crustal levels. Adiabatic incongruent melting occurred at this time, resulting in the partial conversion of original noncellular sodian augite to spongy cellular nonsodian augite and associated mineral phases. Dilation associated with deformation during cellular melting locally resulted in growth of the coarser boxy-lamellar cellular augite. Fracturing and cleaving reasonably relate to mechanical interaction of phenocrysts during intrusion, and perhaps also to the development of cracking related to the decompression.

This interlude of dissolution melting and incongruent melting was followed by crystallization of the ambient melt as a fine-grained matrix and final crystallization of cell melt. Whether final crystallization was related to a second eruptive pulse, or to development of a steep thermal gradient at a "cold" low-pressure site reached in the main event of decompression, is not known.

ACKNOWLEDGEMENTS

If it were not for the field trip to the Thetford limburgite location, led by Prof. J.B. Lyons in 1958, and for the not more than casual thin sectioning of the collected sample more than 30 years later, revealing the remarkable pyroxene texture, this report would not have been generated. Thanks are extended to the pioneering field work of Warren Chivers, who produced an original location sketch in 1936, and to J.B. Lyons, who found it in the geological archives of Dartmouth College. Line illustrations were prepared by Kris Pizarro. The manuscript was kindly reviewed by Richard C. Bradt, L.S. Hollister, Lung-Chuan Kuo, R.F. Martin, and I.S. McCallum.

REFERENCES

BINNS, R.A. (1969): High-pressure megacrysts in basanitic lavas near Armidale, New South Wales. *Am. J. Sci.* **267-A**, 33-49.

DONALDSON, C.H. (1985): The rates of dissolution of olivine, plagioclase, and quartz in a basalt melt. *Mineral. Mag.* **49**, 683-693.

HADLEY, J.B. (1950): Geology of the Bradford–Thetford area, Orange County, Vermont. *Vt. Geol. Surv. Bull.* **1**.

KUO, LUNG-CHUAN & KIRKPATRICK, R.J. (1985): Kinetics of crystal dissolution in the system diopside – forsterite – silica. *Am. J. Sci.* **285**, 51-90.

LEAVY, B.D. & HERMES, O.D. (1979): Mantle xenoliths from southeastern New England. *In* The Mantle Sample: Inclusions in Kimberlites and Other Volcanics (F.R. Boyd & O.A. Meyer, eds.). Second Int. Kimberlite Conf. Proc. Vol., American Geophysical Union, Washington, **2**, 374-381.

LOFGREN, G.E. (1974): An experimental study of plagioclase crystal morphology: isothermal crystallization. *Am. J. Sci.* **274**, 243-273.

MCHONE, J.G. (1978): Distribution, orientations, and ages of mafic dikes in central New England. *Geol. Soc. Am. Bull.* **89**, 1645-1655.

NELSON, S.T. & MONTANA, A. (1992): Sieve-textured plagioclase in volcanic rocks produced by rapid decompression. *Am. Mineral.* **77**, 1242-1249.

O'BRIEN, H.E., IRVING, A.J. & MCCALLUM, I.S. (1988): Complex zoning and resorption of phenocrysts in mixed potassic mafic magmas of the Highwood Mountains, Montana. *Am. Mineral.* **73**, 1007-1024.

TSUCHIYAMA, A. (1985): Dissolution kinetics of plagioclase in the melt of the system diopside–albite–anorthite, and the origin of dusty plagioclase in andesites. *Contrib. Mineral. Petrol.* **89**, 1-16.

________ & TAKAHASHI, E. (1983): Melting kinetics of a plagioclase feldspar. *Contrib. Mineral. Petrol.* **84**, 345-354.

WILKINSON, J.F.G. (1974): The mineralogy and petrography of alkali basaltic rocks. *In* The Alkaline Rocks (H. Sørensen, ed.). J. Wiley & Sons, New York (67-95).

Received August 25, 1992, revised manuscript accepted September 30, 1993.